JCTC Journal of Chemical Theory and Computation

Toward a General Formulation of Dispersion Effects for Solvation Continuum Models

Ville Weijo,[†] Benedetta Mennucci,[†,‡] and Luca Frediani*,[†]

Centre for Theoretical and Computational Chemistry, Department of Chemistry, University of Tromsø, N-9037 Tromsø, Norway and Department of Chemistry, University of Pisa, Via Risorgimento 35, 56126 Pisa, Italy

Received August 16, 2010

Abstract: We revised the quantum model of Amovilli and Mennucci (*J. Phys. Chem. B* **1997**, *101*, 1051) to include the dispersion contribution to the solvation free energy within the framework of continuum models. Our revised formulation makes use of a single adjustable solvent-dependent parameter, and it can be readily generalized to different quantum mechanical descriptions. In particular, we made use of DFT and applied the model to investigate dispersion effects on vertical excitation energies within a time-dependent DFT framework. Our findings show that dispersion effects constitute a significant component of the absolute solvent effect but when relative solvent−solvent shifts are considered a cancellation effect is observed.

1. Introduction

A faithful description of the molecular properties and processes has to take into account the possible presence of the environment surrounding the system under investigation. This clearly increases the modeling complexity as it is evident when, e.g., the number of interacting subsystems in a liquid solution (chemical processes are almost always involving liquid phases) is considered. In order to tackle such complexity, many strategies have been proposed to simplify the problem. The choice of the specific strategy is dictated by the problem under investigation. In the case of the modeling of electronic structure properties, it is necessary to adopt a quantum-mechanical description of the investigated system, whereas the reminder can be dealt with at a lower level of accuracy. Within this framework, a successful approach is constituted by continuum models, where the environment is described by a structureless medium characterized by a set of parameters in order to model its interactions with the molecular system.

Such interactions are then introduced in the quantum-mechanical description of the molecular system as additional terms in the molecular Hamiltonian operator.[1] The correct description is formally achieved by defining an idealized solvation process, where all interactions are "switched on" from the ideal situation of two infinitely separated systems (the isolated solute and the pure solvent) to the fully interacting system (the solvated molecule). The first step of this ideal process is generally connected to the creation of a cavity in the solvent, where the solute molecule is accommodated. The energy involved in this process is commonly called the cavitation energy. The solute is then placed inside the cavity and allowed to interact electrostatically with the solvent. The electrostatic interaction is a purely classical term, and hence, its expression is well defined within continuum methods. Other nonelectrostatic interactions are intrinsically connected to the quantum nature of both solute and solvent, and it is therefore less obvious how to express them when the solvent is replaced by a continuum. One possible strategy comes from the theory of weakly interacting quantum systems where such interactions are dealt with as small perturbations to the Hamiltonians of the two isolated systems. The main terms in such treatment are called dispersion and repulsion, and they can loosely be connected to the attractive and repulsive terms of the Lennard−Jones (LJ) potential.

The free energy of solvation of a molecular solute can then be expressed as the sum of the above-mentioned contributions

$$G_{sol} = G_{el} + G_{cav} + G_{disp} + G_{rep} \quad (1)$$

where we neglected the contribution due to internal degrees of freedom.

* Corresponding author e-mail: luca.frediani@uit.no.
[†] University of Tromsø.
[‡] University of Pisa.

10.1021/ct1004565
Published on Web 10/21/2010

Historically, most continuum models have been developed to treat the electrostatic contribution to G_{sol}, but several proposals to include nonelectrostatic contributions have been formulated: the interested reader can find a review of the various methodologies developed so far in refs 1 and 2. Most such methodologies focused on reproduction of solvation energies only and they were therefore developed in a semiclassical framework.[3−5]

The growing interest in the modeling of molecular properties that depend on the electronic structure, however, requires the development of a fully quantum mechanical approach to the determination of all solute−solvent interactions, including dispersion and repulsion. In this way both electrostatic and nonelectrostatic energy contributions can be fully integrated in the Hamiltonian operator. Practical expressions for dispersion and repulsion have been developed by Amovilli[6] based on the theory of weak intermolecular forces[7] and later reformulated within the polarizable continuum model[1,2] (PCM) by Amovilli and Mennucci.[8]

This formulation allows for the dispersion and repulsion contributions being included in response property computations. The approach has been used in a coupled perturbed Hartree−Fock (CPHF) framework to compute electronic (hyper)polarizabilities[9] and in a CASSCF framework to obtain vertical excitation energies.[10]

In the present work we will further develop the model by focusing on the dispersion term for which we propose a new parametrization that can easily be adapted to the chosen QM description of the electronic structure. By making use of density functional theory (DFT), we will then apply the method to the calculation of vertical excitation energies within a time-dependent DFT framework.

The paper is organized as follows: in section 2, a brief resume of the theoretical method will be given together with its extension to TDDFT equations. In section 3, the method will be parametrized according to new fitting strategy and it will be applied to study dispersion effects on excitation energies of various small- and medium-sized molecules in different solvents. Finally, in section 4, some conclusive remarks will be given.

2. Methods

2.1. Approximating the Dispersion Term to a Practical Form. Following refs 6 and 8, we begin our approximations by discarding the detailed molecular nature of the solvent and adopting a PCM-like description in terms of apparent surface charge distributions. Within this framework, the dispersion interaction contribution to the solvation Gibbs energy of eq 1 can be defined as

$$G_{\mathrm{disp}} = \frac{1}{\pi}\sum_{ia}\int_0^\infty \mathrm{d}\omega \frac{\Delta\varepsilon_{ai}}{(\Delta\varepsilon_{ai})^2+\omega^2}\int \mathrm{d}\mathbf{r}\int_\Gamma \mathrm{d}\mathbf{s}\rho_{ai}(\mathbf{r})\frac{1}{|\mathbf{r}-\mathbf{s}|}\sigma(\mathbf{s};\rho_{ia},\varepsilon(\mathrm{i}\omega)) \quad (2)$$

where indexes a and i run over the virtual and occupied orbitals of the solute molecule, respectively, $\Delta\varepsilon_{ai}$ is the orbital energy difference between orbitals a and i, Γ refers to the cavity surface, and $\sigma(\mathbf{s};\rho_{ia},\varepsilon(\mathrm{i}\omega))$ is the apparent surface polarization charge at point $\mathbf{s}$ due to the solute transition charge distribution ρ_{ia} and the solvent frequency-dependent dielectric constant $\varepsilon(\mathrm{i}\omega)$ evaluated at the imaginary frequency $\mathrm{i}\omega$.

We further assume that in the case of dispersion, mutual interaction of the induced surface polarization charges does not play a significant role in the solvation energy. This assumption can be justified in light of the fact that dispersion interactions are mostly between two bodies (compare, e.g., to the two-body LJ potential), at least in nonmetallic materials. The surface charges can then be assumed to be proportional to the component of the electric field due to the charge distribution perpendicular to the cavity surface, E_{ia},[8] so that

$$\sigma(\mathbf{s};\rho_{ia},\varepsilon(\mathrm{i}\omega)) = -\frac{\Omega^2}{\Omega^2+\omega^2}\frac{(\eta^2-1)}{4\pi\eta^2}E_{ia}(\mathbf{s}) \quad (3)$$

where η is the refractive index of the continuum at optical frequencies and $\Omega = \eta I$, with I being the first ionization potential of the solvent.

Using eq 3 and denoting the Coulomb potential of the electronic charge distribution ρ_{ia} by V_{ia}, a simplified equation for the dispersion energy defined in eq 2 is obtained

$$G_{\mathrm{disp}} = -\frac{(\eta^2-1)}{8\pi\eta^2}\sum_{ia}\frac{\Omega}{\Omega+\Delta\varepsilon_{ai}}\int_\Gamma \mathrm{d}\mathbf{s}V_{ia}(\mathbf{s})E_{ai}(\mathbf{s}) \quad (4)$$

A further simplification, which is dictated by the need of achieving both an acceptable computational cost and an expression suitable to be used within the SCF framework, is obtained by introducing an averaged excitation energy $\Delta\varepsilon_{\mathrm{ave}}$[8]

$$G_{\mathrm{disp}} = -\frac{(\eta^2-1)}{8\pi\eta^2}\frac{\Omega}{\Omega+\Delta\varepsilon_{\mathrm{ave}}}\int_\Gamma \mathrm{d}\mathbf{s}\sum_{ia}V_{ia}(\mathbf{s})E_{ai}(\mathbf{s}) \quad (5)$$

This expression can be written in terms of occupied and virtual density matrices $\mathbf{P}$ and $\mathbf{Q}$, respectively, in the atomic orbital (AO) basis as

$$G_{\mathrm{disp}} = -\frac{\beta}{2}\sum_{\mu\nu\gamma\delta}P_{\gamma\nu}Q_{\mu\delta}[\gamma\nu|\mu\delta] \quad (6)$$

where μ, ν, γ, and δ refer to AO indices and

$$P_{\gamma\nu} = 2\sum_i^{occ}C_{\gamma i}C_{\nu i} \quad (7)$$

$$Q_{\gamma\nu} = \left(\sum_i^{\mathrm{all}}C_{\gamma i}C_{\nu i} - \sum_i^{occ}C_{\gamma i}C_{\nu i}\right) = S^{-1}_{\gamma\nu} - \frac{1}{2}P_{\gamma\nu} \quad (8)$$

and the symmetrized form of the $V_{\mu\nu}(\mathbf{s})E_{\gamma\delta}(\mathbf{s})$ term is introduced as in the original formulation

$$[\gamma\nu|\mu\delta] = \frac{1}{2}\int_\Gamma \mathrm{d}\mathbf{s}(V_{\gamma\nu}(\mathbf{s})E_{\mu\delta}(\mathbf{s}) + V_{\mu\delta}(\mathbf{s})E_{\gamma\nu}(\mathbf{s})) \quad (9)$$

The factor β is implicitly defined as

$$\beta = \frac{1}{4\pi}\frac{\eta^2 - 1}{\eta^2\left(1 + \frac{\Delta\varepsilon_{ave}}{\Omega}\right)} \quad (10)$$

In the original formulation,[8] the averaged excitation energy $\Delta\varepsilon_{ave}$ was obtained by considering a predefined set of occupied and virtual orbitals defined by a window of energies $[-a, a]$ and averaging for such a set. This choice is, however, strictly connected to the quantum mechanical method employed. In particular, it is well known that DFT and HF descriptions yield very different energies when occupied and virtual orbitals are compared, and the final value for β is strongly dependent on the chosen method.[11] In order to avoid this problem, we propose to use a value of $\Delta\varepsilon_{ave}$ that will yield the same dispersion energies predicted by the "exact" expression in eq 4.

In the original formulation the factor β was scaled by an adjustable parameter c_f replacing the constant $1/4\pi$ with the value $c_f = 0.036$. This value was empirically determined through a comparison with experimental data. In this work we followed a different strategy: we considered the semiclassical dispersion energy values as references and obtained c_f by linear interpolation between adjacent data points (see section 3 for more details).

2.2. SCF Formulation and Its Extension to a Linear Response Approach for Electronic Excitations. Within the SCF approach (here applied at the DFT level of theory), the solvent effect is represented in terms of additional contributions to the Fock matrix of the isolated molecule. In particular, such contributions can be computed by differentiating the corresponding free energy expressions with respect to the orbital parameters (e.g., the density-matrix elements). By adopting the same AO basis expansion used in eq 6, the expression for the dispersion contribution of a closed-shell molecule becomes

$$F_{\mu\nu} = \frac{G_{disp}}{\partial P_{\mu\nu}} = -\frac{\beta}{2}\sum_{\gamma\delta}\left((S^{-1})_{\gamma\delta} - P_{\gamma\delta}\right)[\mu\gamma|\delta\nu] \quad (11)$$

The extension of dispersion interactions to excitation energies is achieved within the TDDFT linear response framework in a similar way as that already done for the electrostatic term.[12−14] The excitation energies of a molecular system are determined by the poles of the linear response function to a time-dependent perturbation, and thus, they can be obtained from the solutions of the non-Hermitian eigensystem[15−17]

$$\begin{bmatrix}\mathbf{A} & \mathbf{B}\\ \mathbf{B} & \mathbf{A}\end{bmatrix}\begin{bmatrix}\mathbf{X}\\ \mathbf{Y}\end{bmatrix} = \omega\begin{bmatrix}\mathbf{1} & \mathbf{0}\\ \mathbf{0} & -\mathbf{1}\end{bmatrix}\begin{bmatrix}\mathbf{X}\\ \mathbf{Y}\end{bmatrix} \quad (12)$$

where the transition vectors (X, Y) correspond to collective eigenmodes of the density matrix with eigenfrequencies ω and the matrices **A** and **B** form the Hessian of the ground-state energy

$$\begin{aligned} A_{ai,bj} &= \delta_{ab}\delta_{ij}(\varepsilon_a - \varepsilon_i) + K^0_{ai,bj}\\ B_{ai,bj} &= K^0_{ai,bj}\end{aligned} \quad (13)$$

where indices $i, j, \ldots$ label occupied, $a, b, \ldots$ virtual, and $s, t, \ldots$ generic molecular orbitals and

$$K^0_{st,uv} = \int d\mathbf{r}\int d\mathbf{r}'\psi^*_s(\mathbf{r}')\psi_t(\mathbf{r}')\left(\frac{1}{|\mathbf{r}' - \mathbf{r}|} + g_{xc}(\mathbf{r}', \mathbf{r})\right)\psi^*_u(\mathbf{r})\psi_v(\mathbf{r}) \quad (14)$$

Here g_{xc} is the exchange-correlation kernel within the adiabatic approximation.

If now we introduce dispersion effects, both **A** and **B** change as follows

$$\begin{aligned} A_{ai,bj} &\Rightarrow A_{ai,bj} + B^{disp}_{ai,bj}\\ B_{ai,bj} &\Rightarrow B_{ai,bj} + B^{disp}_{ai,bj}\end{aligned} \quad (15)$$

$B^{disp}_{ai,bj}$ is the dispersion contribution

$$B^{disp}_{st,uv} = \frac{\beta}{2}[st|uv] \quad (16)$$

which can be obtained from the Fock-operator contribution eq 11. We assume that β remains unchanged with respect to ground-state calculations.

In eq 15 we focused on the dispersion term, but all calculations performed also include the standard PCM electrostatic contribution and the repulsion contribution in both SCF and linear response equations. The interested reader can find detailed derivations of the electrostatic terms from the reference papers.[8,12−14]

3. Results and Discussion

3.1. Computational Details. We computed dispersion energy contributions to solvation and excitation energies of a set of chromophores, including acetone, acrolein, 4-(*N*,*N*-dimethylamino)benzonitrile (DMABN), *p*-nitroaniline (PNA), and the three diazines (pyrazine, pyrimidine, and pyridazine) immersed in cyclohexane and acetonitrile. Molecular geometries were optimized for each solvent and vacuum using the B3LYP[18−20] functional and 6-311G(d,p) basis set.[21] Solvent contributions to geometry optimizations included only electrostatic terms. All calculations were carried out with a local version of the Gaussian 03 program package.[22]

In order to compute dispersion effects on solvation free energies and excitation energies, the DFT and TDDFT approaches have been used in combination with two functionals, the generalized gradient approximation functional PBE[23] and the hybrid B3LYP.[18−20] The dispersion contribution has been shown to be sensitive to basis set quality as discussed in ref 11. On the basis of the results of the reference, we have chosen to use augmented correlation-consistent double-ζ (aug-cc-pVDZ) basis set[24,25] as a good compromise between the size of the set and the accuracy.

The solvent contribution to the dispersion energy contains two solvent-dependent parameters, namely, the refractive index η and the first ionization potential I. We used values of $\eta = 1.424$ and $I = 0.364$ au for cyclohexane and $\eta = 1.344$ and $I = 0.448$ au for acetonitrile.[26]

For all systems, the molecular cavity was obtained as the envelope of spheres centered on selected atoms of the solute, and thus, it is determined by the solute geometry. In the present case, we used cavities constructed by applying the united atom topological model and the atomic radii of the UFF[27] force field as implemented in the Gaussian

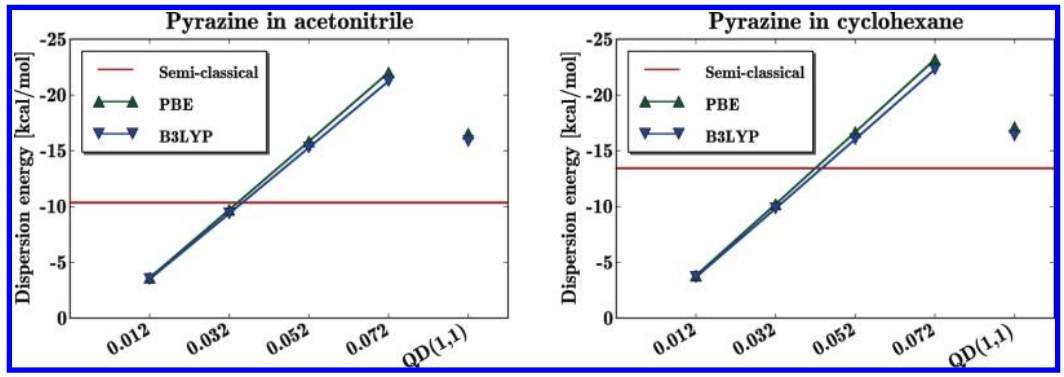

Figure 1. Illustration of the dependence of the dispersion energy on different parametrizations. All values refer to PBE and B3LYP calculations with the aug-cc-pVDZ basis set, 0.012, 0.032, 0.052, and 0.072 refer to different values of c_f (see text for details), and "QD(1.1)" is the value recommended by a previous model. The reference value (represented as an horizontal line) is obtained using a semiclassical method.

code. According to this model, a sphere is associated to each atom (excluding the hydrogens) with a radius defined according to the type of the atom and its bonds. In particular, we have $R(\mathrm{CH}) = 2.125$, $R(\mathrm{C}) = 1.925$, $R(\mathrm{N}) = 1.83$, $R(\mathrm{CH3}) = 2.525$, $R(\mathrm{O}) = 1.75$ (all values are in Angstroms). Semiclassical dispersion energy contributions were parametrized using cavities based on bare Bondi radii, and thus, evaluations of those contributions were made using smaller cavities, where the above-defined radii were divided by 1.2.

3.2. Parameterization. As reported in the Methods section, a proper adjustable parameter was originally introduced by Amovilli and Mennucci in the definition of the factor β, namely

$$\beta = c_f \frac{\eta^2 - 1}{\eta^2\left(1 + \dfrac{\Delta\varepsilon_{\mathrm{ave}}}{\Omega}\right)} \tag{17}$$

with c_f originally set to 0.036.

In order to give an idea of the sensitivity of the method with respect to that parameter, two examples of the behavior of the dispersion energy as a function of parameter c_f are provided in Figure 1, where a pyrazine molecule is placed in two different solvents and its dispersion energy is evaluated. We recall that for each different c_f, the corresponding β factor is obtained using an averaged energy $\Delta\varepsilon_{\mathrm{ave}}$ that yields the same dispersion energy as the "exact" semiclassical value as reported in eq 4. This allows us to eliminate the arbitrary choice of orbitals used in the averaging procedure described in the original formulation.

In both cases, the DFT curves ("PBE" and "B3LYP") are very close to linear, and they have a crossover point with the "semiclassical" reference between the c_f values of 0.032 and 0.052. "QD(1,1) " results, which are based on the previous parametrization of the model ($c_f = 0.036$ and $\Delta\varepsilon_{\mathrm{ave}}$ obtained using the mentioned window of orbital energies for the averaging), are off from the semiclassical values by roughly a factor two. This is most likely because the model was parametrized using the HF method and small basis sets, which are known to produce contributions that are too small when applied to DFT.[11] Results in the figures are illustrative in a sense that the c_f value which makes the dispersion energy equal to the semiclassical value lies between 0.032 and 0.052,

Table 1. Optimal Values for c_f[a]

	acetonitrile		cyclohexane	
	PBE	B3LYP	PBE	B3LYP
acetone	0.04016	0.03407	0.04375	0.04076
acrolein	0.03838	0.03687	0.04724	0.04526
DMABN	0.03725	0.03261	0.04118	0.03688
PNA	0.03690	0.03390	0.04401	0.04132
pyrazine	0.03528	0.03409	0.04356	0.04194
pyridazine	0.03673	0.03546	0.04585	0.04191
pyrimidine	0.03534	0.03419	0.04359	0.04090
optimized values for each solvent and functional				
optimized	0.03690	0.03409	0.04375	0.04132
max. abs. error	0.912	0.775	1.305	2.497
avg. abs. error	0.342	0.275	0.423	0.587
max. rel. error	12.03%	7.62%	7.45%	12.21%
avg. rel. error	3.79%	2.44%	2.84%	3.79%
optimized values for each solvent				
optimized c_f	0.03535		0.04194	
max. abs. error	1.436		2.845	
avg. abs. error	0.539		0.696	
max. rel. error	17.72%		13.92%	
avg. rel. error	4.89%		4.80%	
optimized value (optimized with all the data)				
optimized c_f	0.03726			
max. abs. error	3.071			
avg. abs. error	1.231			
max. rel. error	21.33%			
avg. rel. error	9.53%			

[a] Maximum and average absolute errors are in kcal/mol.

and that the variation of the dispersion energy with respect to c_f is very close to linear. On the basis of these observations, we optimized the value of c_f. The values obtained for different combinations of DFT functionals, solvents, and molecules are shown in Table 1.

Optimal c_f values for each molecule/solvent/functional combination (highest quadrant of the table) were obtained by taking the semiclassical value and interpolating c_f linearly to match the two numbers, and the optimal c_f's are in the range from 0.0326 to 0.04724. Differences in optimal c_f's within a column can be as large as 0.008, which translates to the smallest value being almost one-fifth smaller than the largest one. Such variations of c_f's might seem to be large at first, but it is not evident that those will imply large errors in dispersion energy contributions; thus, we investigated the

possibility of reducing the number of free parameters in our model (from one optimal c_f for each molecule, solvent, and functional).

c_f values for combined data sets were optimized with respect to the sum of relative errors (as compared to the semiclassical values) of individual dispersion contributions. Optimizing the values with respect to the sum of absolute errors has only a minor effect on the optimized values, and thus, these results are not shown here. In addition to the optimized c_f values, we report maximum and average absolute and relative errors obtained when using an optimized c_f in Table 1. Optimized c_f's for solvent/functional combinations are shown in the second quadrant of the table, where we can see that both functionals have optimal c_f's close to each other for a given solvent, optimized values being at most 0.003 apart from each other. The largest absolute errors range from 0.8 to 2.5 kcal/mol, and the average absolute errors range from 0.3 to 0.6 kcal/mol. The largest relative errors are approximately 12%, while the average relative errors are less than 4%. Errors of these magnitudes are certainly acceptable, but it will be interesting to see if we can get rid of the functional specificity of the parametrization in order to be more in line with the idea of a method-independent continuum of PCM.

We optimized c_f values for both solvents by including contributions from both functionals (third quadrant of the table). As expected, errors are now slightly larger than before. Average errors are still very reasonable (0.6−0.7 kcal/mol and 5% for absolute and relative errors, respectively), and maximum absolute errors are 1.4 and 2.8 kcal/mol in acetonitrile and cyclohexane, respectively, which are slightly larger than maximum absolute errors from the previous level of parameter reduction (c_f for each functional/solvent). The parameter reduction can be taken a step further still by optimizing a single c_f value against all data. The results are shown in the fourth quadrant of the table. Using a single c_f value does not change the maximum absolute error much, but average absolute and relative errors roughly double to 1.2 kcal/mol and 10%, respectively. Maximum relative error also increases slightly from the acetonitrile-specific value of 18% to 21%.

As expected, the errors become larger when the number of parameters is reduced. From the point of view of average errors, we conclude that choosing a solvent specific c_f is the most reasonable choice in terms of accuracy and the number of free parameters. This choice fits well within a continuum solvent framework, where the solvent is described by a collection of parameters which determine its interactions with the solute. In order to have a more direct appreciation of the quality of the new solvent-specific parametrization with respect to the semiclassical reference values, we collect both the DFT dispersion energies obtained with solvent-optimized c_f and the corresponding semiclassical values in Table 2.

Table 2. Dispersion Energies (in kcal/mol) with Solvent-Optimized c_f's and Semiclassical (S-C) Reference Values

	acetonitrile		cyclohexane	
	DFT	S-C	DFT	S-C
B3LYP				
acetone	−10.37	−10.35	−12.92	−13.42
acrolein	−10.45	−10.86	−13.04	−14.27
DMABN	−10.36	−10.36	−12.92	−13.43
PNA	−7.32	−7.95	−9.15	−10.32
pyrazine	−6.24	−7.58	−9.38	−9.80
pyridazine	−15.65	−16.65	−20.82	−20.44
pyrimidine	−14.40	−15.03	−18.57	−19.51
PBE				
acetone	−10.74	−10.35	−13.42	−13.42
acrolein	−10.83	−10.86	−14.28	−14.27
DMABN	−10.72	−10.36	−13.81	−13.43
PNA	−7.62	−7.95	−9.56	−10.32
pyrazine	−7.88	−7.58	−10.09	−9.80
pyridazine	−18.09	−16.65	−23.28	−20.44
pyrimidine	−15.69	−15.03	−19.80	−19.51

3.3. Excitation Energies. In this section we extend the analysis of dispersion contributions to excitation energies. In Table 3 we report the values obtained for selected excited states of the same set of molecules used for the previous analysis on solvation free energies. Excitations considered here are the following: the lowest $n-\pi^*$ electronic transition is examined for diazines and acetone, for acrolein both $n-\pi^*$ and $\pi-\pi^*$ excitations are considered, and for PNA and DMABN, charge-transfer excitations (of A symmetry) are studied. In the case of DMABN, the locally excited B2 excitation results are also presented. For each molecule the symmetry of the corresponding excitation is indicated in the tables.

To have a more direct evaluation of the solvatochromic effects obtained by switching on the electrostatic and the dispersion interactions, we report gas-phase electronic excitation energies together with vacuum−solvent energy. There, c_f1 refers to the solvent-optimized value, whereas c_f2 is the globally-optimized coefficient. The QD(1.1) column contains results obtained by using the window parameter of refs 8 and 11, and the ES results are obtained by considering only the electrostatic contribution.

At a first glance, the magnitudes and signs of the solvation shifts might seem to be erratic. However, if the dispersion-included values are compared to the ES values, one sees that dispersion always gives a negative contribution to the corresponding excitation energy. The contributions from our c_f -parametrized models range roughly from −90 to −180 meV, whereas QD(1.1) contributions can be almost twice as large as compared to the corresponding c_f -parametrized shifts.

Depending on the magnitude of the original ES value, dispersion contributions can change the sign of the solvent shift. Magnitudes of dispersion contributions do not change considerably between different solvents, and the c_f1 and c_f2 results are close to each other, at least when comparing to the corresponding ES results. Unfortunately, the accuracy of dispersion-corrected excitation energy shifts is difficult to evaluate as reliable experimental vacuum−solvent excitation energy shift data are difficult to obtain. Experimental solvent−solvent shifts are, however, more readily available. Solvent−solvent excitation energy shifts along with some experimental results are shown in Table 4.

We will first comment on the QD(1.1) and c_f2 values (optimized against all solvent and functional combinations),

Table 3. Computed Vacuum Excitation Energies and Vacuum−Solvent Shifts (all values in eV)[a]

		solvation shift vac−ACN				solvation shift vac−CH			
molecule	vac.	c_f1	c_f2	QD(1.1)	ES	c_f1	c_f2	QD(1.1)	ES
B3LYP									
pyrazine B3U	3.928	−0.094	−0.102	−0.172	0.049	−0.158	−0.137	−0.208	0.020
pyrimidine B1	4.245	0.038	0.030	−0.040	0.181	−0.110	−0.090	−0.159	0.067
pyridazine B1	3.547	0.178	0.169	0.092	0.327	−0.076	−0.056	−0.136	0.107
acetone A	4.415	−0.018	−0.030	−0.098	0.111	−0.161	−0.137	−0.179	0.036
acrolein A″	3.412	−0.026	−0.034	−0.114	0.121	−0.141	−0.120	−0.199	0.043
acrolein A′	5.692	−0.323	−0.331	−0.410	−0.205	−0.314	−0.293	−0.370	−0.161
DMABN B2	4.349	−0.128	−0.135	−0.186	−0.035	−0.164	−0.147	−0.188	−0.033
DMABN A1	4.623	−0.377	−0.385	−0.437	−0.279	−0.314	−0.295	−0.338	−0.175
PNA A	3.892	−0.583	−0.589	−0.660	−0.490	−0.410	−0.393	−0.462	−0.280
PBE									
pyrazine B3U	3.521	−0.102	−0.110	−0.186	0.049	−0.178	−0.156	−0.232	0.011
pyrimidine B1	3.751	0.021	0.013	−0.061	0.171	−0.124	−0.099	−0.174	0.068
pyridazine B1	3.082	0.186	0.177	0.096	0.343	−0.088	−0.063	−0.140	0.121
acetone A	4.245	−0.066	−0.075	−0.119	0.093	−0.175	−0.150	−0.187	0.029
acrolein A″	3.011	−0.037	−0.046	−0.133	0.116	−0.152	−0.130	−0.216	0.042
acrolein A′	5.456	−0.242	−0.251	−0.338	−0.117	−0.240	−0.218	−0.304	−0.085
DMABN B2	3.961	−0.163	−0.171	−0.215	−0.046	−0.200	−0.179	−0.216	−0.040
DMABN A1	4.314	−0.404	−0.412	−0.458	−0.280	−0.347	−0.325	−0.364	−0.179
PNA A	3.512	−0.456	−0.463	−0.539	−0.348	−0.368	−0.349	−0.423	−0.222

[a] ACN marks acetonitrile and CH cyclohexane.

Table 4. Computed Acetonitrile−Cyclohexane Solvent Shifts with Experimental Results (all values in eV)

molecule	func.	c_f1	c_f2	QD(1.1)	ES	exp.
pyrazine B3U	B3LYP	0.064	0.035	0.036	0.029	0.040[a]
	PBE	0.076	0.046	0.046	0.038	
pyrimidine B1	B3LYP	0.148	0.119	0.119	0.114	0.120[a]
	PBE	0.145	0.112	0.113	0.103	
pyridazine B1	B3LYP	0.254	0.225	0.228	0.220	0.260[a]
	PBE	0.274	0.240	0.236	0.222	
acetone A	B3LYP	0.142	0.107	0.081	0.075	0.06[b]
	PBE	0.109	0.074	0.069	0.064	
acrolein A″	B3LYP	0.115	0.085	0.085	0.078	
	PBE	0.115	0.084	0.084	0.075	
acrolein A′	B3LYP	−0.009	−0.039	−0.039	−0.045	
	PBE	−0.002	−0.033	−0.034	−0.032	
DMABN B2	B3LYP	0.036	0.012	0.002	−0.003	
	PBE	0.036	0.008	0.001	−0.005	
DMABN A1	B3LYP	−0.064	−0.090	−0.099	−0.104	−0.20[c]
	PBE	−0.058	−0.087	−0.094	−0.100	
PNA A	B3LYP	−0.173	−0.196	−0.197	−0.210	−0.13[d]
	PBE	−0.088	−0.114	−0.116	−0.125	

[a] Acetonitrile−isoctane, ref 28. [b] Acetonitrile−*n*-hexane, ref 29. [c] Reference 30. [d] Acetonitrile−dichloromethane, ref 31.

which are reasonably close to each other in most cases, acetone's B3LYP value being a small exception. The similarity of the QD(1.1) and c_f2 results comes from the fact that they use the same prefactor for both solvents, and the difference between the solvents is only obtained from the variations of the parameters of the permittivity at imaginary frequencies (see eq 3). For both solvents, the parameters η and I are almost the same, and consequently, without different prefactors, the excitation energy shift should be more or less the same. This implies that the solvent−solvent shifts should be small for QD(1.1) and c_f2 results, and indeed, this can be observed from Table 4, where inclusion of dispersion contributions through QD(1.1) and c_f2 creates a positive solvent−solvent shift of roughly 0.01 eV or less, which can be considered small as compared to the magnitude of ES solvent−solvent shifts in most cases. As expected by the differences in prefactors, c_f1 solvent−solvent shifts are larger than those obtained with c_f2 and the differential effect is, in most cases, a positive further shift of approximately 0.03 eV.

Experimental data on Table 4 are scattered as they were not available for all chromophore/solvent combinations, and in some cases we reported data obtained in similar solvents. For all available data, differences between dispersion-corrected and ES shifts are quite small and they both are in relatively good agreement with experiments.

Finally, from the combined analysis of the two tables we observe that dispersion effects on relative solvatochromic shifts are small for all excitations and systems studied. This is in agreement with previous studies based on a different methodology.[32] It is therefore not possible to make a final assessment of the different parametrizations. On the other hand, larger differences are observed when absolute shifts (with respect to vacuum) are considered: the old parametrization when applied to TDDFT calculations seems to overestimate the dispersion contribution, while the new proposed scheme yields corrections to the electrostatic values which are more balanced. This confirms that the combined use of "optimal" averaged energy $\Delta\varepsilon_{ave}$ and c_f parameter is a robust approach to extend the dispersion model to different QM levels of description.

4. Conclusions

We revised the quantum-mechanical formulation of the dispersion contribution to the solvation energy within the context of the polarizable continuum model originally proposed by Amovilli and Mennucci.[8] The parametrization of the model, which avoids the approximated estimate of the averaged energy $\Delta\varepsilon_{ave}$ entering in the definition of the dispersion energy, is now achieved through a single parameter c_f used to "scale" the overall dispersion contribution. For the present work, c_f has been fitted to reproduce the dispersion energy values obtained with a highly parametrized semiclassical model. It turns out that the optimal strategy is

to select a different c_f for each solvent. Moreover, this new parametrization scheme does not show the large sensitivity to the QM level of calculation found in the original formulation, and therefore, it represents a promising method to extend the dispersion formulation to other QM descriptions.

We also employed optimized c_f values to compute the dispersion contribution to electronic excitation energies. The obtained net effect due to dispersion is a red shift for all the investigated systems in the two solvents employed. Our findings show that dispersion is a significant contribution to the overall solvent effect, but unlike the electrostatic contribution, it does not depend strongly on the specific solvent. As a result, if one is interested in solvatochromic shifts, i.e., changes of excitation energies passing from one solvent to the other, results obtained with the electrostatic model often yield satisfactory results in comparison to experimental shifts due to the almost exact cancellation of the dispersion contributions.

Acknowledgment. The support of the IT department of the University of Tromsø for computational resources is greatly acknowledged. L.F. and V.W. acknowledge the Tromsø Forskningsstiftelse for financial support.

References

(1) Tomasi, J.; Mennucci, B.; Cammi, R. *Chem. Rev.* **2005**, *105*, 2999.

(2) Tomasi, J.; Persico, M. *Chem. Rev.* **1994**, *94*, 2027.

(3) Floris, F. M.; Tomasi, J.; Ahuir, J. L. P. *J. Comput. Chem.* **1991**, *12*, 784–791.

(4) Cramer, C. J.; Truhlar, D. G. *Acc. Chem. Res.* **2008**, *41*, 760–768.

(5) Soteras, I.; Curutchet, C.; Bidon-Chanal, A.; Orozco, M.; Luque, F. J. *J. Mol. Struct.:THEOCHEM* **2005**, *727*, 29–40.

(6) Amovilli, C. *Chem. Phys. Lett.* **1994**, *229*, 244–249.

(7) Amovilli, C.; McWeeny, R. *Chem. Phys. Lett.* **1986**, *128*, 11–17.

(8) Amovilli, C.; Mennucci, B. *J. Phys. Chem. B* **1997**, *101*, 1051–1057.

(9) Mennucci, B.; Amovilli, C.; Tomasi, J. *Chem. Phys. Lett.* **1998**, *286*, 221–225.

(10) Cossi, M.; Barone, V. *J. Chem. Phys.* **2000**, *112*, 2427–2435.

(11) Curutchet, C.; Orozco, M.; Luque, F. J.; Mennucci, B.; Tomasi, J. *J. Comput. Chem.* **2006**, *27*, 1769.

(12) Cammi, R.; Mennucci, B.; Tomasi, J. *J. Phys. Chem. A* **2000**, *104*, 5631.

(13) Cammi, R.; Mennucci, B. *J. Chem. Phys.* **1999**, *110*, 9877.

(14) Cossi, M.; Barone, V. *J. Chem. Phys.* **2001**, *115*, 4708.

(15) Bauernschmitt, R.; Ahlrichs, R. *Chem. Phys. Lett.* **1996**, *256*, 454.

(16) Stratmann, R. E.; Scuseria, G. E.; Frisch, M. J. *J. Chem. Phys.* **1998**, *109*, 8218.

(17) Hirata, S.; Head-Gordon, M. *Chem. Phys. Lett.* **1999**, *314*, 291.

(18) Becke, A. D. *J. Chem. Phys.* **1993**, *98*, 5648.

(19) Lee, C.; Yang, W.; Parr, R. G. *Phys. Rev. B* **1988**, *37*, 785.

(20) Stephens, P. J.; Devlin, F. J.; Chabalowski, C. F.; Frisch, M. J. *J. Phys. Chem.* **1994**, *98*, 11623.

(21) Krishnan, R.; Binkley, J. S.; Seeger, R.; Pople, J. A. *J. Chem. Phys.* **1980**, *72*, 650.

(22) Frisch, M. J.; Trucks, G. W.; Schlegel, H. B.; Scuseria, G. E.; Robb, M. A.; Cheeseman, J. R.; Montgomery, J. A., Jr.; Vreven, T.; Kudin, K. N.; Burant, J. C.; Millam, J. M.; Iyengar, S. S.; Tomasi, J.; Barone, V.; Mennucci, B.; Cossi, M.; Scalmani, G.; Rega, N.; Petersson, G. A.; Nakatsuji, H.; Hada, M.; Ehara, M.; Toyota, K.; Fukuda, R.; Hasegawa, J.; Ishida, M.; Nakajima, T.; Honda, Y.; Kitao, O.; Nakai, H.; Klene, M.; Li, X.; Knox, J. E.; Hratchian, H. P.; Cross, J. B.; Bakken, V.; Adamo, C.; Jaramillo, J.; Gomperts, R.; Stratmann, R. E.; Yazyev, O.; Austin, A. J.; Cammi, R.; Pomelli, C.; Ochterski, J. W.; Ayala, P. Y.; Morokuma, K.; Voth, G. A.; Salvador, P.; Dannenberg, J. J.; Zakrzewski, V. G.; Dapprich, S.; Daniels, A. D.; Strain, M. C.; Farkas, O.; Malick, D. K.; Rabuck, A. D.; Raghavachari, K.; Foresman, J. B.; Ortiz, J. V.; Cui, Q.; Baboul, A. G.; Clifford, S.; Cioslowski, J.; Stefanov, B. B.; Liu, G.; Liashenko, A.; Piskorz, P.; Komaromi, I.; Martin, R. L.; Fox, D. J.; Keith, T.; Al-Laham, M. A.; Peng, C. Y.; Nanayakkara, A.; Challacombe, M.; Gill, P. M. W.; Johnson, B.; Chen, W.; Wong, M. W.; Gonzalez, C.; Pople, J. A. *Gaussian 03*; Gaussian, Inc.: Wallingford, CT, 2004.

(23) Perdew, J. P.; Burke, K.; Ernzerhof, M. *Phys. Rev. Lett.* **1996**, *77*, 2865.

(24) T. H. Dunning, J. *J. Chem. Phys.* **1989**, *90*, 1007.

(25) Kendall, R. A.; T. H. Dunning, J.; Harrison, R. J. *J. Chem. Phys.* **1992**, *96*, 6796.

(26) In *Handbook of Chemistry and Physics*, 91st ed.; Lide, D. R., Ed.; CRC Press: Boca Raton, FL, 2009.

(27) Rappe, A.; Casewit, C.; Colwell, K.; Goddard, W.; Skiff, W. *J. Am. Chem. Soc.* **1992**, *114*, 10024.

(28) Baba, H.; Goodman, L.; Valenti, P. C. *J. Am. Chem. Soc.* **1966**, *88*, 5410.

(29) Renge, I. *J. Phys. Chem. A* **2009**, *113*, 10678–10686.

(30) Lipinski, J.; Chojnacki, H.; Grabowski, Z. R.; Rotkiewicz, K. *Chem. Phys. Lett.* **1980**, *70*, 449–453.

(31) Moran, A. M.; Kelley, A. M. *J. Chem. Phys.* **2001**, *115*, 912–924.

(32) Li, J.; Cramer, C. J.; Truhlar, D. G. *Int. J. Quantum Chem.* **2000**, *77*, 264–280.

CT1004565